Void Fraction and Pressure Drop in Two-Phase Equilibrium Flows in a Vertical 2×3 Rod Bundle Channel — Assessment of Correlations against the Present Subchannel Data*

Michio SADATOMI**, Keiko KANO**, Akimaro KAWAHARA** and Naoki MORI**

In order to increase void fraction and pressure drop data in a multi-subchannel system like an actual fuel rod bundle, air-water experiments have been conducted using a vertical 2×3 rod bundle channel made up of two central and four side subchannels as the test channel. Void fraction and pressure drop in each subchannel were measured and the frictional pressure drop was determined mainly for slug and churn flows. The results show that both the void fraction and the frictional pressure drop are higher in the central subchannel than the side one. In order to analyze the data, the data on gas and liquid flow rates in each subchannel under the same flow condition have been used. In the analysis, the calculations by various correlations reported in literatures have been compared with the present data for validation. The recommended correlations respectively for the void fraction and the frictional pressure drop have been clarified. Results of such experiments and analyses are presented and discussed in this paper.

***Key Words*:** Multiphase Flow, Nuclear Reactor, Flow Measurement, Void Fraction, Pressure Drop, Subchannel, Rod Bundle

1. Introduction

Subchannel analysis is a familiar method to predict thermal and hydraulic behavior of coolant in a fuel rod bundle in boiling water nuclear reactors (BWR). However, the reliability of the analysis is not perfect. So, studies aiming at the improvement of the analysis are still continuing, e.g., Ninokata et al.(1) In order to improve it, accurate experimental data are necessary to validate it especially for a multi-subchannel system like a fuel rod bundle. Studies by Lahey et al.(2),(3) were the pioneering works which presented experimental data on flow distribution in two-types of multi-subchannel systems. Unfortunately, however, the data for other flow parameters, such as fluid transfer between subchannels, pressure drop and void fraction in each subchannel etc., were not obtained.

In our previous studies in this series, experiments and analyses have been conducted for two-phase flows in a vertical 2×3 rod bundle channel made up of two central and four side subchannels. Turbulent mixing rate between the subchannels(4), flow distribution and flow characteristics(5), prediction of the distribution in annular flow for hydraulically equilibrium flows(6), and flow redistribution due to void drift for the non-equilibrium flows(7) had been studied. Following these, void fraction and pressure drop in each subchannel have been measured and analyzed in the present study in order to obtain more reliable prediction method for these parameters. In the experiments, air and water were used as the working fluids, and the data were obtained for bubbly, slug, churn, and annular flows, but the major regimes were slug and churn flows. In the analyses, several correlations of the void fraction and the frictional pressure drop reported in literatures have been tested against the present data. Results of such experiments and analyses are described in this paper.

* Received 1st September, 2005 (No. 05-4153)

** Department of Mechanical System Engineering, Graduate School of Science and Technology, Kumamoto University, 2–3–1 Kurokami, Kumamoto-city 860–8555, Japan.
E-mail: sadatomi@mech.kumamoto-u.ac.jp

Nomenclature

Symbol Description Unit

D_h : Hydraulic diameter of subchannel m
F : Force per unit control volume N/m^3
j : Volumetric flux m/s
P : Pressure Pa
u : Mean velocity m/s
Z : Axial distance m

Greek Symbols

α : Volume fraction –
ε : Relative error = (Cal – Exp)/Exp –

ε_{ABS} : Absolute error = (Cal − Exp) −
ρ : Density kg/m^3

Subscripts

Cal : Calculation
Exp : Experiment
f : Frictional component
g : Gravitational component
G : Gas
I : Gas-liquid interface
L : Liquid
RMS : Root-mean-square value
M : Mean value
W : Wall
1, 2, i : Subchannel identifier

All the parameters without a subchannel identifier refer to those for the whole channel made up of six subchannels.

2. Experiment

Figure 1 show the cross-section of the test channel. The channel had six subchannels, i.e., two central and four side subchannels, by inserting two full rods and four half rods, both 16 mm O.D., in a 40 mm × 44 mm rectangular duct. The gap clearance between the two rods and that between the rod and the duct wall were all 4.0 mm. The hydraulic diameter and the flow area of each subchannel and the channel as a whole are listed in an attached table. The walls of the brass full rods and the transparent acrylic half rods and duct were hydraulically smooth. A pin spacer of 2.0 mm O.D. was inserted every 0.5 m in the axial positions to support the full rod. In addition, the diameter of the rods was enlarged from those in actual BWR to prevent vibrations.

The flow loop of the vertical test channel, shown in Fig. 2, is almost the same as that used in our previous studies[(4)–(7)]. The test channel consisted of four main sections, i.e., 1.25 m entry, 0.75 m tracer injection, 2.25 m mixing and 0.5 m discharge sections, and the total length was 5.0 m. Water and air at ambient temperature and pressure were introduced into three subchannel groups, i.e., Ch.1-1 group and two Ch.2-2 groups, from the bottom end of the entry section. The flow rates of water and air in each group were so controlled for the flow in the mixing section to become hydraulically equilibrium flow, as described in Sadatomi et al.[(5)] In the mixing section, both phases could go through all the gaps between the subchannels. In the other three sections, however, they could not because of the insertion of 1.0 mm thick fins into the grooves on the duct and the rods walls, as shown in the left hand side of the figure.

The difference from the previous test section was the insertion of a test section with paired quick shut valves at both ends into the mixing section. In the test section, mean void fractions in the three subchannel groups were measured with the quick shut valve method, and the mean value of the two Ch.2-2 groups was taken as the mean void fraction in Ch.2 because of the symmetry of the flow. The valves were simultaneously operated with a pair of solenoids within about 0.1 s. In order to obtain accurate void fraction data within the uncertainty of ±1% in reading, the operations were repeated 15 to 30 times depending upon the flow condition. Besides the void fraction, the total pressure drop and the system pressure at the test section was measured with a differential-type and a gauge-type pressure transducers within the uncertainties of ±1% and ±2% in reading. The frictional component of the pressure drop in subchannel i, $(\Delta P_f/\Delta Z)_i$, was obtained by

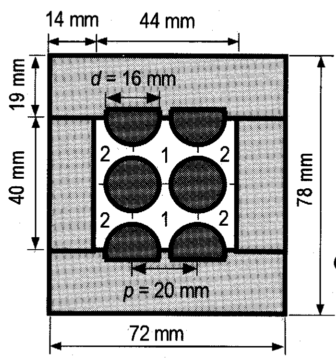

	Hydraulic dia. D_h mm	Flow area A mm^2
Ch.1	14.3	194
Ch.2	11.2	138
Whole	12.3	941

Gap size: $S_{11} = S_{12} = S_{22} = 4.0$ mm

Fig. 1 Cross-section of the test channel with 2×3 rods

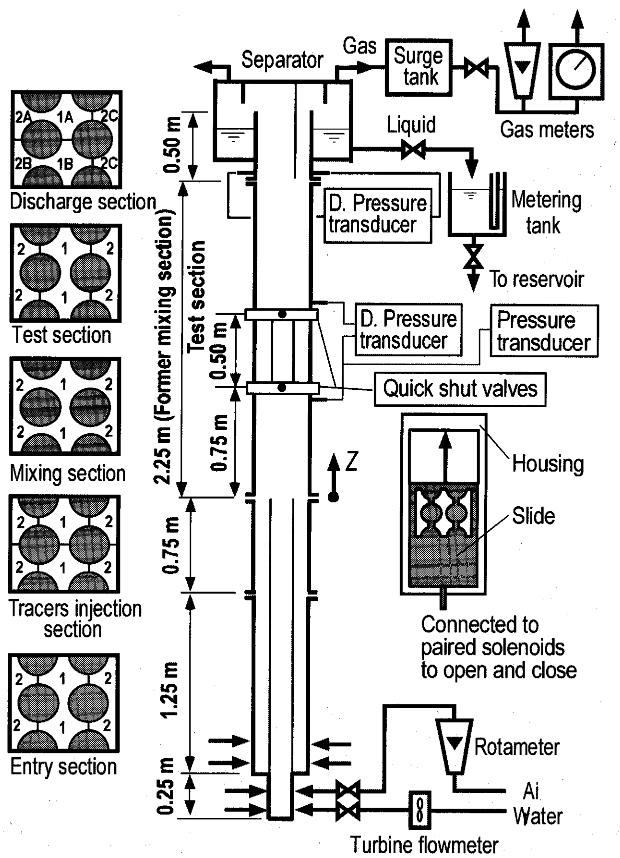

Fig. 2 Flow loop of the test channel with 2×3 rods

neglecting the acceleration component and inserting the measured total pressure drop, ΔP_i, and the volume fraction, α_{ki} ($k = G$ for the gas phase and $k = L$ for the liquid phase), into:

$$|\Delta P_f/\Delta Z|_i = |\Delta P/\Delta Z|_i - (\rho_G\alpha_{Gi} + \rho_L\alpha_{Li})g. \quad (1)$$

The uncertainty of the frictional pressure drop data was estimated to be within 5%.

In addition, some pictures were taken with a high-speed video camera and a digital camera to determine the flow regime. The ranges of volumetric fluxes of air and water in the channel as a whole were $0.1 \le j_G \le 35$ m/s and $0.1 \le j_L \le 2.0$ m/s. The flow regimes covered were bubbly, slug, churn, and annular flows. The number of data points in each flow regime is 11 in bubble flows, 25 in slug and churn flows and 7 in annular flows.

3. Experimental Results

3.1 Flow rates of both phases in each subchannel

Figure 3 shows typical flow distribution data in a hydraulically equilibrium two-phase flow at $j_L = 1.0$ m/s[5]. The ordinate is the ratio of flow rates in one subchannel to the whole channel. The data points are plotted with different symbols depending on the phases and the subchannels, i.e., Ch. 1A, 1B and 2C. Bubble flow to slug and churn flow transition occurred at nearly the same j_G in both subchannels, and the transition line is drawn on the figure. In bubble flows, the ratios for the both phases are similar to those in single-phase flow. In slug and churn flows, the ratio of gas phase in Ch. 1A and 1B is higher than that in single-phase flow and the ratio of liquid phase is lower, and vice versa in Ch. 2C. This means that the larger subchannel is rich in the gas and poor in the liquid while the smaller one is poor in the gas and rich in the liquid. In annular flows, the ratios approach to those in single-phase flow again though the data are not seen in this figure. The trend of such data is quite similar to those reported by Lahey et al.[2],[3] In addition, we could confirm the symmetry of the flow from Ch. 1A and 1B data. So, the data in Ch. 1A and 1B were averaged and the averaged value was used in the following discussions.

3.2 Void fraction in each subchannel

Figure 4 shows void fraction data for Ch.1 and 2 against j_G at $j_L = 1.0$ m/s. Corresponding to the flow distribution data mentioned above, the void fraction of Ch.1, is higher than that of Ch.2 especially in slug-churn flow region of $j_G > 0.35$ m/s. A similar trend was also observed under other j_L conditions though the related data are not plotted to minimize confusion. This data trend agrees with the calculations by Carlucci et al.'s correlations[8]. However, the agreement is not quantitatively enough as reported by Sadatomi et al.[5]

3.3 Total pressure drop in each subchannel

Figure 5 shows total pressure drop data in each subchannel. The pressure drop is almost identical between Ch.1 and Ch.2 because the flow under consideration is a hydraulically equilibrium flow in which both the pressure difference and the net fluid transfer do not exist between the subchannels as a time averaged value.

3.4 Frictional pressure drop in each subchannel

Figure 6 shows frictional pressure drop data in each

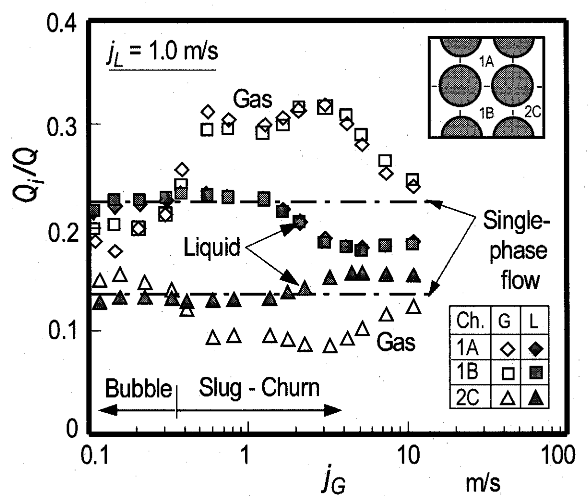

Fig. 3 Flow distribution data in a hydraulically equilibrium two-phase flow at $j_L = 1.0$ m/s[5]

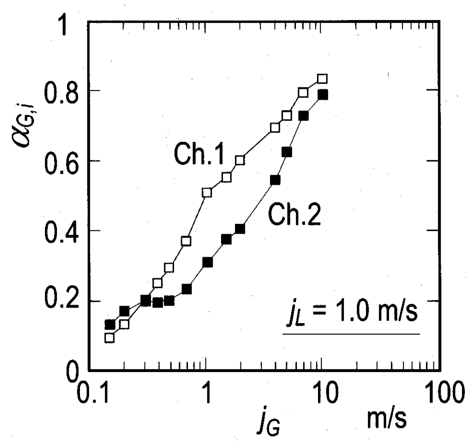

Fig. 4 Void fraction data in each subchannel at $j_L = 1.0$ m/s

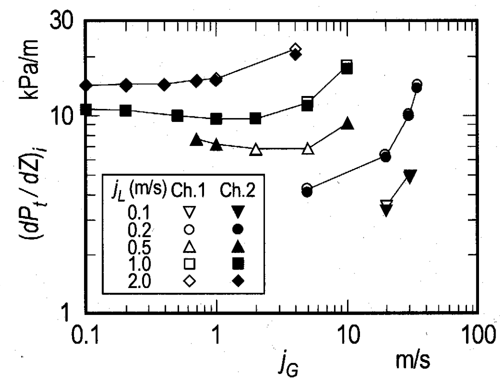

Fig. 5 Total pressure drop data in each subchannel

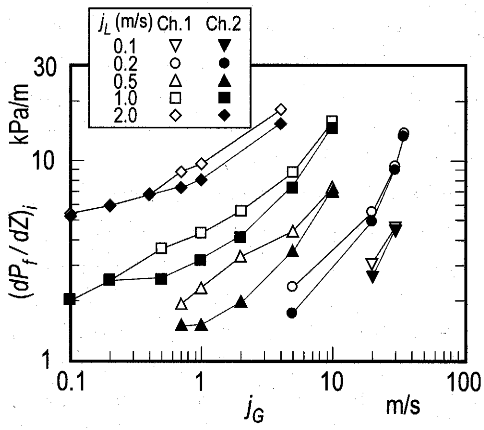

Fig. 6 Frictional pressure drop data in each subchannel

subchannel. The frictional pressure drop is higher in Ch.1 than Ch.2 especially in slug and churn flows as is expected from the void fraction and the total pressure drop data. The general trend of the data is identical between the present channel and circular pipe data, i.e., the frictional pressure drop increases with j_G and j_L.

4. Assessment of Correlations

4.1 Void fraction in each subchannel

Tables 1 and 2 respectively show assessment results for 7 correlations in traditional two-phase mixture models (Dix(9), Chisholm(10), Chen-Spedding(11), Bestion(12), Inoue(13), Mishima-Hibiki(14), Maier-Coddington(15)) and in the well-known two-fluid models (TRAC-PF1/MOD1 by Liles et al.(16), RELAP5/MOD2 by Ransom et al.(17), and their modifications by changing the combination of wall and interfacial friction correlations). The correlations in Table 1 were selected by considering the assessment results by Coddington-Macian(18), and the combinations in Table 2 by considering the assessment results by Sadatomi et al.(7) Here, the definitions of the mean absolute error, $\varepsilon_{ABS,M}$ and the RMS absolute error, $\varepsilon_{ABS,RMS}$ are as follows:

$$\varepsilon_{ABS,M}=\sum_{j}^{N}\varepsilon_{ABS,j}\Big/N, \quad (2)$$

$$\varepsilon_{ABS,RMS}=\sqrt{\sum_{j}^{N}\varepsilon_{ABS,j}^{2}\Big/(N-1)}. \quad (3)$$

In the calculation of two-fluid model (See Appendix for details), 6 combinations of the wall friction force, F_{WL}, including separated flow correlation in Chierici et al.'s version(19) and the interfacial friction force, F_I were tested. However, when RELAP5/MOD2 was used for the calculation of the interfacial friction force, the solution and therefore ε_{ABS} were not obtained in a void fraction range of $0.64<\alpha_G<0.79$. So, the total number, N, in Eqs. (2) and (3) in that case was less than other cases.

In the mixture model, Dix's correlation gives the best prediction for both Ch. 1 and Ch. 2 data, and Chisholm's and Inoue's ones are the second best respectively for Ch. 1 and Ch. 2 data. In the two-fluid model, the combination of RELAP5 for F_{WL} and TRAC for F_I gives the best prediction for both Ch. 1 and Ch. 2 data, and that of the separated flow correlation for F_{WL} and TRAC for F_I is the second best.

Figure 7(a)–(d) compares the experiment with the calculations by Dix's correlation in the mixture model, and the combinations of the original TRAC-TRAC, the original RELAP5-RELAP5 and the RELAP5-TRAC in the two-fluid model. In the Dix's correlation, all the data points are within the error band of ±0.1 regardless of j_L and the subchannel. In the RELAP5-TRAC combination, the agreement in $0.4<\alpha_{Gi}<0.7$ became better than those for the original TRAC-TRAC and the RELAP5-RELAP5.

Table 1 Assessment of mixture model in void fraction prediction

Correlations	$\varepsilon_{ABS,M}$		$\varepsilon_{ABS,RMS}$	
	Ch.1	Ch.2	Ch.1	Ch.2
Dix	0.004	0.025	0.033	0.042
Chisholm	0.015	0.041	0.039	0.063
Chen- Spendding	0.011	0.037	0.041	0.061
Bestion	-0.067	-0.055	0.093	0.078
Inoue	-0.007	-0.003	0.056	0.050
Mishima-Hibiki	-0.001	0.027	0.052	0.062
Maier-Coddington	-0.049	-0.045	0.089	0.084

Table 2 Assessment of two-fluid model in void fraction prediction

Wall friction	Interfacial friction	$\varepsilon_{ABS,M}$		$\varepsilon_{ABS,RMS}$	
		Ch.1	Ch.2	Ch.1	Ch.2
TRAC	TRAC	0.028	0.029	0.064	0.068
RELAP5	RELAP5	0.026	0.010	0.093	0.088
TRAC	RELAP5	0.053	0.047	0.089	0.093
RELAP5	TRAC	0.006	0.003	0.052	0.056
Separated	TRAC	0.018	0.019	0.058	0.061
Separated	RELAP5	0.037	0.020	0.084	0.074

4.2 Frictional pressure drop in each subchannel

Tables 3 and 4 respectively show assessment results,

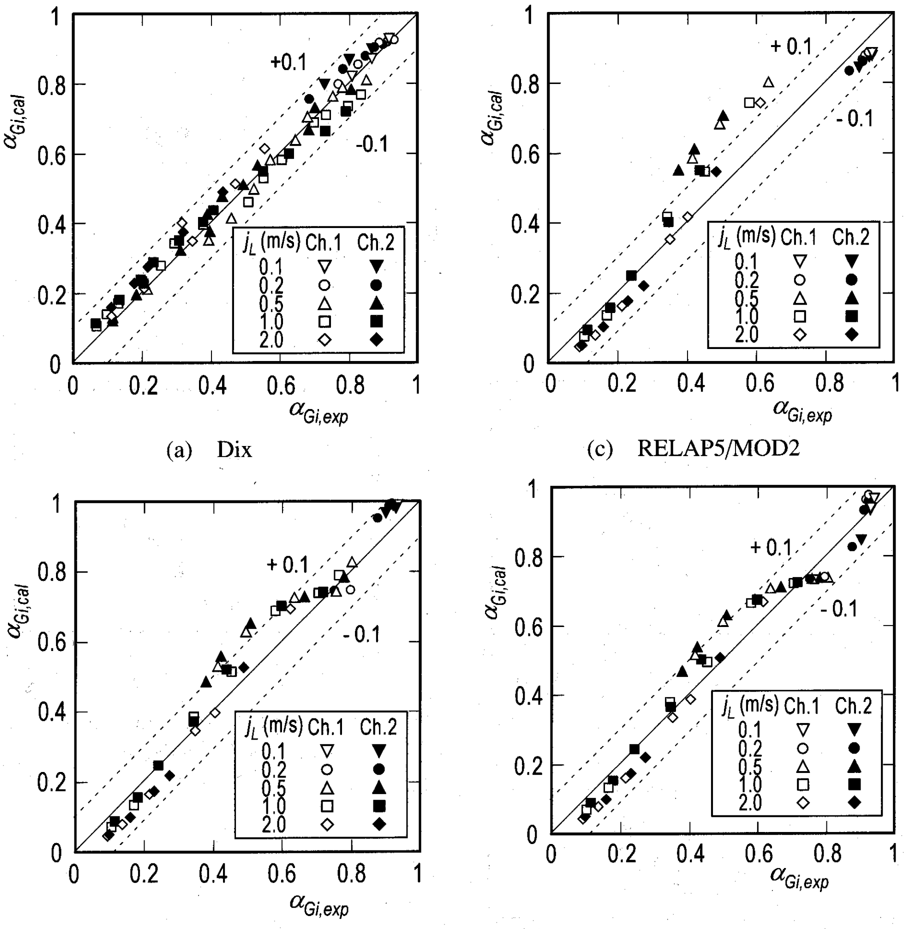

(a) Dix

(c) RELAP5/MOD2

(b) TRAC-PF1/MOD1

(d) RELAP5 and TRAC respectively for F_{WL} and F_I

Fig. 7 Assessment of void fraction prediction

Table 3 Assessment of mixture model in frictional pressure drop prediction

Correlations	ε_M %		ε_{RMS} %	
	Ch.1	Ch.2	Ch.1	Ch.2
Homogeneous (McAdams)	-27.8	-20.4	30.7	26.9
Homogeneous (Dukler et al.)	-42.7	-36.3	44.8	38.1
Homogeneous (Beattie-Whalley)	-33.0	-25.2	34.9	28.0
Separated (Chierici et al.)	-20.3	-12.6	**29.0**	**25.1**
Chisholm	-32.7	-29.2	35.7	33.7
Storek-Brauer	1.0	8.8	23.0	27.0

Table 4 Assessment of two-fluid model in frictional pressure drop prediction

Wall friction	Interfacial friction	ε_M %		ε_{RMS} %	
		Ch.1	Ch.2	Ch.1	Ch.2
TRAC	TRAC	-54.6	-52.1	57.7	54.5
RELAP5	RELAP5	311	199	551	271
TRAC	RELAP5	-34	-34.7	85.1	82.7
RELAP5	TRAC	382	265	682	383
Separated	TRAC	64.5	20.2	190	70
Separated	RELAP5	-3.6	-11.6	**35.7**	**25.9**

i.e., the mean relative error, ε_M, and the RMS relative error, ε_{RMS}, for 6 correlations in the mixture models (Homogeneous flow correlations with different mixture viscosities by McAdams[20], Dukler et al.[21] and Beattie-Whalley[22], separated flow correlation in Chierici et al.'s version[19], Chisholm[23] and Storek-Brauer[24]) and for the 6 combinations in the two-fluid models. The correlations in Table 3 were selected by referring to the previous assessments in our laboratory.

In the calculation of single-phase or two-phase homogeneous friction factor, the effects of subchannel geometry

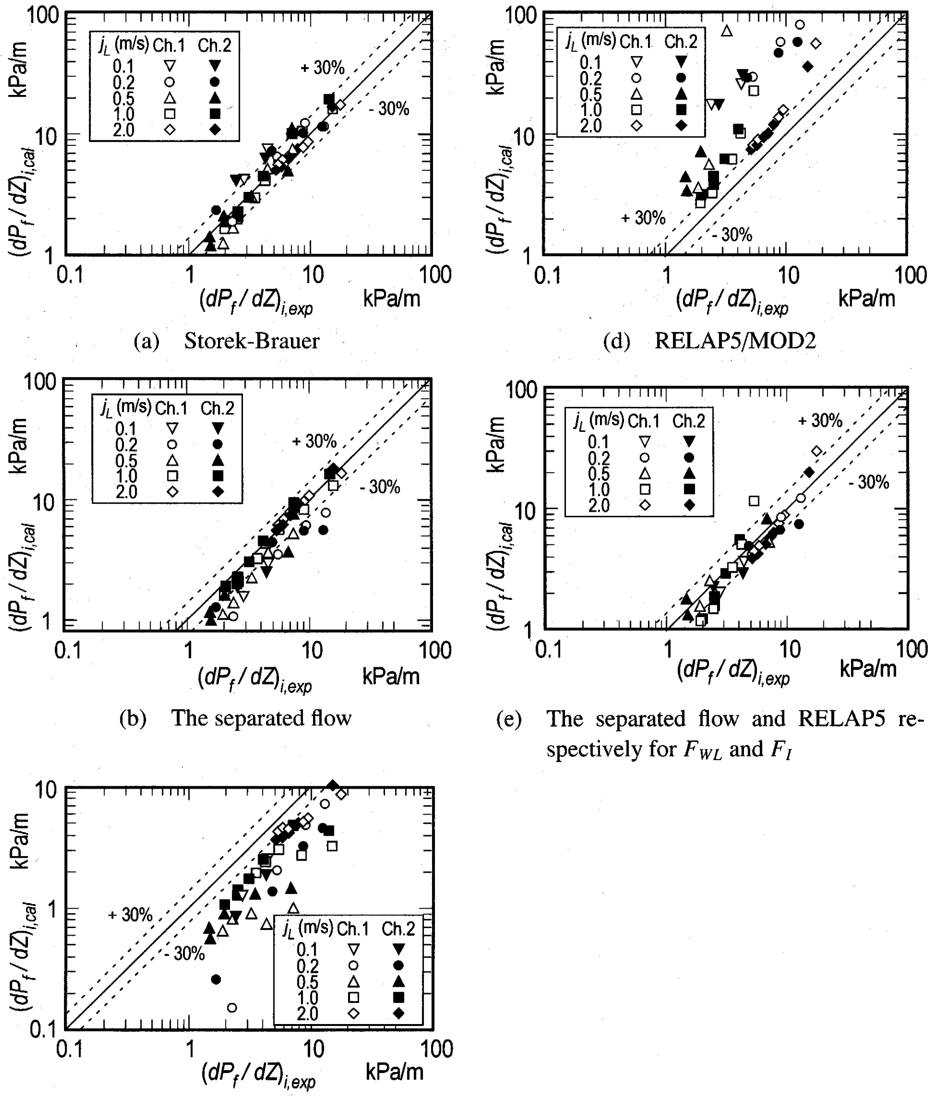

(a) Storek-Brauer

(d) RELAP5/MOD2

(b) The separated flow

(e) The separated flow and RELAP5 respectively for F_{WL} and F_I

(c) TRAC-PF1/MOD1

Fig. 8 Assessment of frictional pressure drop prediction

were taken into account by a Sadatomi et al.'s geometry factor[25] whenever possible.

In the mixture model, Storek-Brauer's and the separated flow correlations are the best respectively for Ch.1 data and for Ch.2 data. In the two-fluid model, the separated flow-RELAP5 combination is the best for both Ch.1 and Ch.2 data.

Figure 8 (a)–(e) compares the experiment with the calculations by Storek-Brauer's and the separated flow correlations in the mixture model, and the combinations of the original TRAC-TRAC, the original RELAP5-RELAP5 and the separated flow-TRAC in the two-fluid model. In Storek-Brauer's correlation, most data points are within the error band of ±30% regardless of j_L and the subchannels. The separated flow correlation under-predicts about 20% the data. The original TRAC-PF1/MOD1 under-predicts considerably the data while the original RELAP5/MOD2 over-predicts. In comparison with the original TRAC-PF1/MOD1 and the original RELAP5/MOD2, the combination of the separated flow-RELAP5 shows extremely good agreement.

4.3 Total pressure drop in each subchannel

The best correlations in the mixture model and the best and the second best combinations of F_{WL} and F_I in the two-fluid model in the sections 4.1 and 4.2 were used to calculate the total pressure drop in each subchannel.

$$|\Delta P_t/\Delta Z|_i = |\Delta P_f/\Delta Z|_i + (\rho_G \alpha_{Gi} + \rho_L \alpha_{Li})g. \qquad (4)$$

Figure 9 (a)–(c) is the results of the comparison between the experiment and the calculations. In Fig. 9 (a), Dix's correlation and Storek-Brauer's one respectively for α_G and $\Delta P_f/\Delta Z$ were used in the mixture model, and the agreement is roughly within ±30%. In Fig. 9 (b), the separated flow correlation and RELAP5/MOD2 respectively for F_{WL} and F_I were used in the two-fluid model, and the agreement is within ±30% besides one point. These two cases are the best respectively in the mixture and the two-

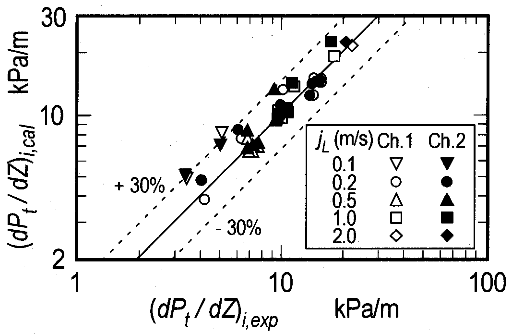

(a) Dix and Storek-Brauer respectively for α_{Gi} and $(\Delta P/\Delta Z)_{fi}$

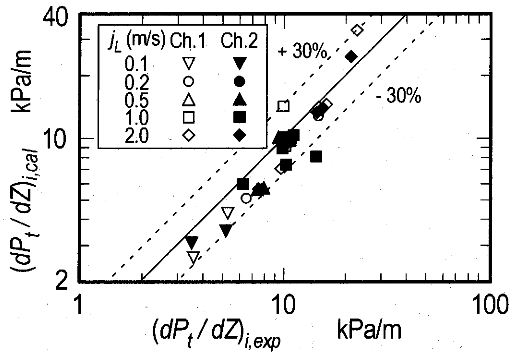

(b) The separated flow and RELAP5 respectively for F_{WL} and F_I

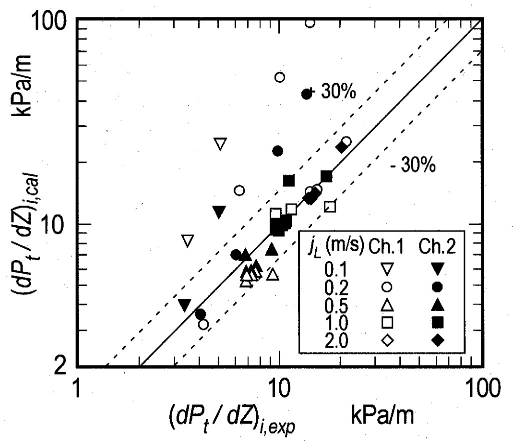

(c) The separated flow and TRAC-PF1 respectively for F_{WL} and F_I

Fig. 9 Assessment of total pressure drop prediction

fluid models. In Fig. 9 (c), the result is shown for the separated flow-TRAC-PF1/MOD1 for F_{WL} and F_I in the two-fluid model. Although the combination of the separated flow-TRAC-PF1/MOD1 gave the second best agreement in the void fraction prediction, the agreement is poor in the total pressure drop prediction. The poverty must be caused by the inaccuracy in the frictional pressure drop prediction seen in Table 4.

5. Conclusions

In order to increase the void fraction and the pressure drop data in each subchannel in a multi-subchannel system under hydraulic equilibrium flow conditions, experiments have been conducted with water and air as the working fluids and a vertical 2×3 rod bundle as the test channel. By analyzing the data, the followings have been clarified.

(1) Both the void fraction and the frictional pressure drop are higher in the central subchannel than the side one especially in slug and churn flows.

(2) The void fraction data in each subchannel could be best predicted by Dix's correlation in the mixture model and the combination of RELAP5-TRAC for F_{WL}-F_I (wall friction force - interfacial friction force) in the two-fluid model.

(3) The frictional pressure drop data could be best predicted by Storek-Brauer's correlation in the mixture model and the combination of separated flow-RELAP5 for F_{WL}-F_I in the two-fluid model.

(4) The total pressure drop data could be best predicted by Dix's void fraction and Storek-Brauer's frictional pressure drop correlations in the mixture model and by the combination of the separated flow-RELAP5 for F_{WL}-F_I in the two-fluid model.

Acknowledgements

The authors gratefully acknowledge Mr. Y. Minesaki and Mr. J. Nakao for their cooperation in the experiments and technicians in the machine shop of the Faculty of Engineering at Kumamoto University for their cooperation in manufacturing the quick shut valves as well as the test channel.

Appendix

For calculating the void fraction and the frictional pressure drop in each subchannel, say Ch.i, by a one-dimensional two-fluid model (Ishii and Mishima[26]) for an adiabatic flow, the following momentum equations for the respective phases were solved simultaneously:

$$\frac{d}{dZ}\left(\rho_G\alpha_{Gi}u_{Gi}^2\right)+F_{Ii}+F_{gGi}+\alpha_{Gi}\frac{dP_{Gi}}{dZ}=0, \quad (5)$$

$$\frac{d}{dZ}\left(\rho_L\alpha_{Li}u_{Li}^2\right)+F_{WLi}-F_{Ii}+F_{gLi}+\alpha_{Li}\frac{dP_{Li}}{dZ}=0. \quad (6)$$

Here, the first term in the left hand side of these equations was very small in comparison with other terms, thus neglected. The wall friction force for the gas phase, F_{WGi}, could be taken to be zero in the present experimental range. The gravitational forces for the gas and the liquid phases, F_{gGi} and F_{gLi}, could be determined from the volume fractions, α_{Gi} and α_{Li}. Thus, the correlations of the wall friction force for the liquid phase per unit volume (= frictional pressure drop), F_{WLi}, and the interfacial friction force per unit volume, F_{Ii} were required to solve the equations. Therefore, we tested several correlations in Tables 2 and 4 as a trial.

In addition, since the flow under consideration is a vertical adiabatic flow, a condition of equal pressure drops between the phases,

$$\delta E_i = \frac{dP_{Gi}}{dZ} - \frac{dP_{Li}}{dZ} = 0, \qquad (7)$$

has to be satisfied as a closure equation. Actually, the calculation was iterated by a numerical method called "Binary method" until δE_i in Eq. (7) became less than 50 Pa/m by changing the void fraction, α_{Gi}.

References

(1) Ninokata, H. et al., Development of Generalized Boiling Transition Model Applicable for Wide Variety of Fuel Rod Bundle Geometries — Basic Strategy and Numerical Approaches, Proc. of GENES4/ANP2003, September 15-19, Kyoto, Japan, (2003), 10 pages in CD-ROM.

(2) Lahey Jr., R.T. et al., Out-of-Pile Sub-Channel Measurements in a Nine Rod Bundle for Water at 1000 PSIA, Edited by Hestroni, G., Progress in Heat and Mass Transfer, Vol.6 (1972), pp.345–363, Pergamon Press, London.

(3) Sterner, R.W. and Lahey Jr., R.T., Air/ Water Subchannel Measurements of the Equilibrium Quality and Mass-Flux Distribution in a Rod Bundle, US DOE Report, NUREG/CR-3373, (1983).

(4) Sadatomi, M. et al., Single-and Two-Phase Turbulent Mixing Rate between Adjacent Subchannels in a Vertical 2×3 Rod Array Channel, Int. J. Multiphase Flow, Vol.30 (2004), pp.481–498.

(5) Sadatomi, M. et al., Flow Characteristics in Hydraulically Equilibrium Two-Phase Flows in a Vertical 2×3 Rod Bundle Channel, Int. J. Multiphase Flow, Vol.30 (2004), pp.1093–1119.

(6) Kawahara, A. et al., Prediction of Flow Distribution in Gas-Liquid Two-Phase Annular Flows in a Rod Bundle under Hydraulically Equilibrium Condition, Proc. of ASME FEDSM'03 4th ASME-JSME Joint Fluid Engineering Conference, July 6–10, Honolulu, Hawaii, USA, (2003), 7 pages in CD–ROM.

(7) Sadatomi, M. et al., Two-Phase Void Drift Phenomena in a 2×3 Rod Bundle — Flow Redistribution Data and Their Analysis, Proc. of the 10th International Topical Meeting on Nuclear Reactor Thermal Hydraulics (NURETH-10), October 5–9, Seoul, Korea, (2003), 18 pages in CD-ROM.

(8) Carlucci, L.N., Hammouda, N. and Rowe, D.S., Two-Phase Turbulent Mixing and Buoyancy Drift in Rod Bundles, Nuclear Engineering and Design, Vol.227 (2004), pp.65–84.

(9) Dix, G.E., Vapor Void Fraction for Forced Convection with Subcooled Boiling at Low Flow Rates, Rep. NEDO-10491, (1971), General Electric Co.

(10) Chisholm, D., Void Fraction during Two-Phase Flow, J. Mechanical Engineering Science, Vol.15 (1973), pp.235–236.

(11) Chen, J.J.J. and Spedding, P.L., An Extension of the Lockhart-Martinelli Theory of Two-Phase Pressure Drop and Hold-Up, Int. J. Multiphase Flow, Vol.7 (1981), pp.659–675.

(12) Bestion, D., The Physical Closure Laws in the CATHARE Code, Nuclear Engineering and Design, Vol.124 (1990), pp.229–245.

(13) Inoue, A. et al., In-Bundle Void Measurement of a BWR Fuel Assembly by an X-Ray CT Scanner: Assessment of BWR Design Void Correlation and Development of New Void Correlation, Proc. of the ASME/JSME Nuclear Engineering Conference, Vol.1 (1993), pp.39–45.

(14) Mishima, K. and Hibiki, T., Some Characteristics of Air-Water Two-Phase Flow in Small Diameter Vertical Tubes, Int. J. Multiphase Flow, Vol.22 (1996), pp.703–712.

(15) Maier, D. and Coddington, P., Review of Wide Range Void Correlations against and Extensive Data Base of Rod Bundle Void Measurements, Proc. of 5th International Conference on Nuclear Engineering (ICONE-5), May 26–30, Nice, France, (1997), Paper No.2434.

(16) Liles, D.R. et al., TRAC-PF1/MOD1 Correlations and Models, NUREG/CR-5069, LA-11208-MS, Los Alamos National Laboratory, New Mexico, USA, (1988).

(17) Ransom, V.H. et al., RELAP5/MOD2 Code Manual, Vol.1: Code Structure, System Models, and Solution Methods, NUREG/CR-4312, EGG-2796, EG&G Idaho, Inc., Idaho, USA, (1985).

(18) Coddington, P. and Macian, R., A Study of the Performance of Void Fraction Correlations Used in the Context of Drift-Flux Two-Phase Flow Models, Nuclear Engineering and Design, Vol.215 (2002), pp.199–216.

(19) Chierici, G.L., Ciucci, G.M. and Slocchi, G., Two-Phase Vertical Flow in Oil Wells — Prediction of Pressure Drop, J. Petroleum Technology, Vol.26 (1974), pp.927–938.

(20) McAdams, W.H. et al., Vaporization Inside Horizontal Tubes: II, Benzen-Oil Mixtures, Trans. ASME, Vol.64 (1942), pp.193–200.

(21) Dukler, A.E., Wicks, M. and Cleveland, R.G., Pressure Drop and Holdup in Two-Phase Flow, AIChE J., Vol.10 (1964), pp.38–51.

(22) Beattie, D.R.H. and Whalley, P.B., A Simple Two-Phase Frictional Pressure Drop Calculation Method, Int. J. Multiphase Flow, Vol.8 (1982), pp.83–87.

(23) Chisholm, D., A Theoretical Basis for the Lockhart-Martinelli Correlation for Two-Phase Flow, Int. J. Heat Mass Transfer, Vol.10 (1967), pp.1767–1778.

(24) Storek, H. and Brauer, H., Reibungsdruckverlust der Adiabaten Gas/Flüssigkeit-strömung in Horizontalen und Ventikalen Rohren, VDI Forschungsheft, Vol.599 (1980), pp.1–36.

(25) Sadatomi, M., Sato, Y. and Saruwatari, S., Two-Phase Flow in Vertical Noncircular Channels, Int. J. Multiphase Flow, Vol.8 (1982), pp.641–655.

(26) Ishii, M. and Mishima, K., Two-Fluid Model and Hydrodynamic Constitutive Relations, Nuclear Engineering and Design, Vol.82 (1984), pp.107–126.